Original Article

Sent to the Corner: xylem vessel anatomy not surface area determines megaphyll hydraulics in *Cecropia obtusa* Trécul (Urticaceae)

Running title: **Xylem vessel anatomy not surface area determines megaphyll hydraulics**

Sébastien Levionnois[1*], Sabrina Coste[2], Eric Nicolini[3], Clément Stahl[4], Hélène Morel[5], Patrick Heuret[4*]

1. CNRS, UMR EcoFoG (AgroParisTech, CIRAD, CNRS, INRA, UA, UG), 97379 Kourou Cedex France.
2. UG, UMR EcoFoG (AgroParisTech, CIRAD, CNRS, INRA, UA, UG), 97379 Kourou Cedex France.
3. CIRAD, UMR AMAP (CIRAD, CNRS, INRA, IRD, Université Montpellier II), 34398 Montpellier, France.
4. INRA, UMR EcoFoG (AgroParisTech, CIRAD, CNRS, INRA, UA, UG), 97379 Kourou Cedex France.
5. CIRAD, UMR EcoFoG (AgroParisTech, CIRAD, CNRS, INRA, UA, UG), 97379 Kourou, France.

*Authors for correspondence:
Sébastien Levionnois, PhD student
Postal address: UMR EcoFog, Campus Agronomique, Avenue de France
BP709 – 97387 Kourou Cedex
French Guiana
Tel: +33 760 26 73 83
Email: sebastien_levionnois@live.fr

Patrick Heuret, PhD
Postal adress: UMR EcoFog, Campus Agronomique, Avenue de France
BP709 – 97387 Kourou Cedex
French Guiana
Tel: +33 694 38 12 19
Email: patrick.heuret@inra.fr

Author contributions

P.H. designed and lead the project; P.H., S.L., E.N., S.C., H.M. and C.S. collected field samples and measured morphological traits; S.L. realized the anatomical cuts and images analysis; S.L. and P.H performed data analysis; S.L. and P.H. wrote the paper; all authors discussed the results and commented on.

Abstract

- Corner's rule predicts a positive correlation between leaf dimensions and the cross-sectional area of the primary stem. Although this relationship is usually explained by hydraulic and mechanical requirements, these hypotheses have never been tested empirically. Corner's rule is also tricky to investigate since rapid secondary growth of the stem prevents a rigorous link being established between a given leaf and the supporting stem. We chose a twig-like leaf model since petiole anatomy is only linked to the attached lamina. We then tested the hypothesis that anatomical adjustments to hydraulic requirements related to vessel size enable reduced investment in tissue in the framework of Corner's rule.
- We conducted an extensive functional, mechanistic and intraspecific investigation of *Cecropia obtusa* Trécul, a Neotropical pioneer tree, by integrating morphological, anatomical and theoretical hydraulic traits around the lamina-petiole size relationship.
- The twig-like structure of the leaf and the strong lamina-petiole correlation of this model tree species made it possible to use a leaf-level model for a relevant investigation of the functional implications of Corner's rule. We found a positive correlation between petiole size, lamina size, the ratio of mean vessel area to vessel frequency in the petiole xylem and theoretical specific conductivity in the petiole xylem.
- Hydraulic function supports Corner's rule to a lesser extent than previously thought. Variations in vessel dimensions drive xylem hydraulic performances and avoid disproportionate petiole cross-sections relative to the lamina.

Key words: allometry, *Cecropia obtusa*, Corner's rules, hydraulic, intraspecific, leaf-stem relationship, petiole anatomy, lamina-petiole relationship

INTRODUCTION

Trees are complex organisms that rely on multi-embedded hierarchical levels of organization, from cells to tissues and organs (Barthélémy and Caraglio, 2007). However, in competition for light, a tree must be viewed as a dynamic system where at every ontogenetic step the plant is able to improve thanks to its previously acquired structure. Owing to these structures, the success of trees is closely linked to several key functions including exploration, assimilation, conduction, mechanical support, defense or reproduction. During the life history of a tree, its intrinsic constraints and needs continuously change with size as well as with the micro-environment (e.g. irradiance, competition). To maintain the different functions and hence performances, coordination and adjustment to the different structures is required continuously through both ontogeny and environmental variation. In this context, carbon gain and allocation are main issues since they determine possible adjustment, investment, optimization and benefit. Thus, considering tree development from the point of view of the organization and coordination of cells, tissues and organs is a precondition for understanding the mechanisms that enable maximum carbon gain.

At the organ level, leaves have received a great deal of attention because of the major role they play in the plant carbon economy thanks to photosynthesis. At the interspecific level, the currently widely accepted paradigm relates to a global spectrum of leaf economy, running from quick to slow returns on investments (Wright et al., 2004). Because leaf surface area encompasses six orders of magnitude (Milla and Reich, 2007; Niinemets et al., 2007), the leaf-stem relationship (LSR) continues to be a good way to improve our understanding of such variability. From an evolutionary perspective, in his seminal paper on “Durian Theory” E.J.H. Corner already made empirical observations such as “The stouter the main stem, the bigger the leaves and the more complicated their form” (Corner, 1949). He completed this with a second point he called “diminution on ramification” as “The greater the ramification, the smaller become the branches and their appendages”. These principles were referred to as Corner’s rules by Hallé *et al.* (Hallé et al., 1978) and have been explored by several authors (White, 1983a; b; Brouat et al., 1998; Brouat and McKey, 2001; Preston and Ackerly, 2003; Westoby and Wright, 2003; Sun et al., 2006; Normand et al., 2008; Liu et al., 2010). However, from a more developmental point of view, even before Corner, by drawing attention to the pith, E.W. Sinnott (Sinnott, 1921) suggested that the size of organs (the stem, leaf, fruit) is correlated with the size of the meristem from which they develop. Nevertheless, both at the intra- and interspecific level, the relationship between stem and leaf size is frequently and intuitively explained by functional requirements in terms of hydraulic and

mechanical supplies (Hallé et al., 1978; White, 1983a; b; Brouat et al., 1998; Westoby and Wright, 2003; Normand et al., 2008). Since the respective contributions of the hydraulic and mechanical functions have not yet been tested, there is a need to (i) explore the diversity of anatomical structures that lead to interspecific variation in the LSR and (ii) understand the anatomical adjustments that allow for variations in the size of the stem and of the leaf at the intraspecific level (Lehnebach et al., 2018). The aim of this study was thus to investigate the intraspecific mechanisms of the LSR from the point of view of hydraulics and the aforementioned carbon allocation issues.

The hydraulic explanation for LSR is not simple. In angiosperms, xylem vessels drive water conduction through the soil-plant-atmosphere continuum (Tyree and Zimmermann, 2002) according to the cohesion-tension theory (Dixon and Joly, 1895; Steudle, 2001). Vessel dimensions vary considerably at interspecific level (Chave et al., 2009; Zanne et al., 2010; Olson and Rosell, 2013), at intraspecific level (Lens et al., 2011; Hajek et al., 2016) and at the intra-individual level (Anfodillo et al., 2006, 2013; Bettiati et al., 2012; Schuldt et al., 2013), with dramatic consequences for hydraulic performance at the organ, individual, population or species levels (Hacke et al., 2016). According to the Hagen-Poiseuille law (Tyree and Zimmermann, 2002), vessel hydraulic conductivity is a fourth-power function of the vessel diameter. Thus, even slight variations in vessel diameter have dramatic impacts on associated conductance. A greater or lesser water demand with respect to the leaf lamina surface can theoretically be satisfied either by increasing the surface area of the conductive tissues which supply it, or by modifying the conductivity of the related tissues by means of their anatomy. Therefore, we hypothesize that adjustments to stem vessel size first drive size-related hydraulic supplies, thereby limiting over-increments of xylem with an increase in leaf size. Consequently, even if stem xylem surface areas are positively correlated with leaf size, the hydraulic function explains the LSR to a lesser extent than previously thought.

However, focusing on the leaf-stem system is hampered by several technical limitations. One of the main difficulties in applying a rigorous approach to the LSR is defining where to sample the last elongated shoot. On one hand, Corner (Corner, 1949) refers to primary diameter (Hallé et al., 1978), which means that no secondary growth has occurred. Secondary growth occurs very soon, possibly at the same time as the elongation process, meaning LSR may vary over time. On the other hand, the internode of a first-year shoot supplies not only the leaf at its apex, but all the leaves supported by internodes distal to it as well as the bud content (Cochard et al., 2005). It would thus be more relevant to analyze the relationship between the total surface area of leaves borne by the first-year shoot and the

cross-sectional area of the shoot (Brouat et al., 1998). A compromise for a functional assessment would be to shift to a leaf-level model (i.e. considering the petiole to be homologous to the stem and its associated lamina), since there are plant groups in which the differences between leaf and shoot, or more precisely between the petiole and the stem remain fuzzy (Givnish, 1984; Poorter and Rozendaal, 2008; Nicotra et al., 2011). Indeed, compound or double-compound leaves, or large palmate or palmatilobate leaves look like more to a branch in a physiognomic or functional sense. Using a leaf model to investigate the LSR makes it possible to avoid the bias frequently encountered at the phytomer level. Indeed (i) a petiole strictly supports mechanical and hydraulic constraints associated with its single lamina since it represents the closest structure to the transpiring compartments (Bucci et al., 2003) and (ii) even if a petiole undergoes secondary growth, the growth still only concerns the functional requirements of the associated lamina. Consequently, using a leaf model would make it possible to focus on petiole or venation traits, for instance, and to rigorously investigate the functional implications of the LSR. Finally, the lamina-petiole relationship has already been proven to be a relevant tool for functional investigations, and, for instance, (Royer et al., 2007) showed that this relationship is a significant predictor for inferring fossil functional traits.

In this context, the genus *Cecropia* (Urticaceae), an iconic pioneer tree in the Neotropics, could provide several consistent tree models to improve our understanding of structure-function relationships. These plants have a simple architecture (Heuret et al., 2002; Zalamea et al., 2008) with few botanical entities (e.g. axes, leaves), but have large petioles, reaching more than 1 m in length and up to 2 cm in diameter (Fig. 1b). Linked to its heliophilous habit, petioles have a somewhat branching function (Givnish, 1984; Poorter and Rozendaal, 2008) and can be considered as axes, since the hydraulic and mechanical features of petioles are comparable to a branch with respect to the form of the leaf (palmatilobate to palmate megaphylls with numerous lobes tens of centimetres in length) and its size (up to 0.4 m^2 for *Cecropia obtusa* Trécul with 1-m long petiole).

Here, we provide a functional assessment of intraspecific LSR in *Cecropia obtusa* by focusing on the lamina-petiole relationship in the megaphyll and its hydraulic implications. First, we report an extensive investigation of the relationships between leaf-level traits to validate the lamina-petiole relationship. We hypothesize that, at this level, correlation properties are comparable to the LSR, thereby enabling further functional assessment. Second, after providing the first description of the anatomy of the petiole, we focus on the lamina-petiole relationship by integrating, according to leaf size (i) the surface areas and

proportions of the different component tissues of the petiole, (ii) structural anatomical traits such as the number of xylem vessels, their hydraulic-weighted dimensions and their frequency, and (iii) theoretical hydraulic traits (derived from the Hagen-Poiseuille law) such as hydraulic conductivity and xylem- or leaf-specific hydraulic conductivity.

MATERIALS AND METHODS

Study site

This study was conducted in French Guiana along a forestry road in Counami (N5.41430°, W53.17547°, geodesic system WGS84) where the entrance to the road is located 5 km to the east of Iracoubo municipality. The warm wet tropical climate of French Guiana is highly seasonal due to the north-south movement of the Inter-Tropical Convergence Zone. Annual rainfall is 3041 mm year^{-1} and annual mean air temperature is 25.7 °C at Paracou experimental station (Gourlet-Fleury et al., 2004). There is one long dry season lasting from mid-August to mid-November, during which rainfall is < 100 mm month^{-1}.

Plant material, sampling and morphological measurements

In order to explore a wide range of leaf sizes, we studied 25 adult trees (Fig. 1a) and four juvenile trees. Juvenile trees were less than 2.2 m in height and by counting the number of nodes along the trunk (Heuret et al., 2002; Zalamea et al., 2012), their age was estimated at between 8 and 13 months. The dimensions of adult trees ranged from 10.9 to 22.6 m in height, 6.21 to 30.49 cm in diameter at breast height, and the trees were from 7 to 21 years old. Juvenile trees were studied in September 2014. Adult trees were felled regularly from September 2014 to October 2016, between 0800 am and 1030 pm. After felling, all the axes of the crown were tagged according to their position in the tree architecture and all the leaves were tagged according to which axis they belonged, and their rank from the apex. All the leaves in the crown were cut by sectioning the petiole as close as possible to its insertion point on the stem and immediately placed in plastic bags and then in coolers. One to five leaves per tree -hereafter called P-leaves- just fully expanded and positioned on the 3rd or 4th nodes located under any apex, were put aside for the anatomical studies.

To enable a full understanding of the study, here we recall certain plant morphology prerequisites. *Cecropia* leaves are palmatilobate (Fig. 1b and 2). Consequently, there is no single midrib but as many midribs as there are lobes, i.e. a midrib departs from each lobe. We use the term lamina to refer to the flat thin photosynthetic part of the leaf. We use the term petiole to refer to the physical connection between the lamina and the stem. Finally, we use

the term leaf to refer to the global structure composed of a petiole and a lamina. In the laboratory, all the leaves were processed at the same time of day to keep them as fresh as possible. The petioles were cut as close to the lamina as possible. The length of the petiole (L_{pet}, cm) and two median and orthogonal diameters (mm) of each petiole were measured (Fig. 2a). From these two diameters, a cross-sectional area was derived in the shape of an ellipse (A_{pet}, mm²; Fig. 2a). For each lamina, the length of the main lobe (i.e. the largest one in the continuation of the petiole; LM_{lobe}, cm) was measured and the number of lobes (N_{lobe}) counted (Fig. 2b, c). Exactly 2.851-cm² of lamina in the form of three tablets were sampled with a circular iron punch (diameter = 1.1 cm) taking care to avoid main nerves (Fig. 2d). In the P-leaves, two 1-cm-long petiole segments in the median position were sampled and weighed (Fig. 2e, f). The first segment was used to measure their specific density, expressed as the ratio of dry mass to the fresh volume (PSG: Petiole Specific Gravity; (Williamson and Wiemann, 2010); Table 1). The fresh volume of the sample was calculated using an inverse Archimedes principle and a precision balance (CP224S, Sartorius), as the difference between the fresh mass and immersed mass of the sample. Dry mass was derived after drying at 103 °C for three days. The second segment was preserved in 70° alcohol and later used for anatomical measurements (see the section headed 'Anatomical and hydraulic measurements').

Lamina area (A_{lamina}, cm²; Fig. 2g) was measured with a planimeter (LiCor 3000A, LiCor Inc., Lincoln, NE, USA). The condition of the lamina (damaged or undamaged) was described. Each leaf (leaf + petiole + 3 tablets) was dried at 70 °C for 72 hours. The dry mass of the petiole (M_{pet}, g), the lamina (M_{lamina}, g) and the three tablets_taken together (g) was measured with a precision scale. The lamina mass area (LMA, g cm^{-2}) was derived from the ratio of the dry mass to the known surface area of the three tablets (Fig. 2a).

Data from 2112 mature fully-developed leaves (P and non-P-leaves) were used for morphological validation of the LSR. When we analyzed relationships, including lamina area, we only considered leaves with undamaged lamina (n = 1072). We also investigated the branching intensity-stem size trade-off (Osada et al., 2015), considering lobes (i.e. main nerves) as homologues of the branching process, and by studying the ratio of the number of lobes to the undamaged lamina area (number of lobes per lamina unit area, we refer to as "lobing" intensity; n mm^{-2}) according to the leaf size.

Anatomical and hydraulic measurements

Because anatomical studies are time consuming, we conducted our study on a subset of 60 P-leaves selected to represent (i) our 29 individual trees to minimize individual effects and (ii)

the range including the largest petiole diameters (from 2.59 to 15.41 mm). Anatomical transversal cross-sections, 20 to 50 µm thick, were sampled from the petiole segments with a manual microtome (Mikrot L, Schenkung Dapples, Switzerland). All cross-sections were stained in a safranin/astra-blue solution to color unlignified cells blue and lignified cells red.

Each cross-section corresponding to a given petiole was digitized with an optical microscope (Olympus BX60; Olympus Corporation; Tokyo; Japan) with x50 magnification and a Canon camera EOS 500D (lens Olympus U-TVI-X ; F 0.0; ISO 100; speed 1/25). Three or four close ups were taken of a petiole part at different depths of focus and stacked with the Helicon Focus software (v.6.3.2.Pro, http://heliconsoft.com/). Output pictures were assembled in a panorama using Kolor AutoPanoGiga software (v.3.0.0, http://kolor.com/autopano/) to obtain a complete picture of the cross-section. The digitized cross-sections were processed with CS5 Photoshop software (v.12.0, http://adobe.com/products/photoshop/html). We distinguished eight tissue categories that comprise the petiole anatomy (see anatomical description in the 'Results' section). We manually delineated the tissues on the photographs and created layer masks. The masks of these layers were used to calculate the surface area of each tissue and the whole petiole area with the ImageJ software (v.1.43u; http://imagej.nih.gov/ij/). For the xylem, the cropped part of the image in which the vessels were visible was also analyzed with the ImageJ software to calculate theoretical xylem hydraulic properties (Abramoff et al., 2004). For each vessel, we calculated its surface area (μm^2) and its elliptical diameters. These data were used to derive all the anatomical and hydraulic traits listed in Table 1. To study variations in the dimensions of the vessel, we used the mean hydraulic diameter (Dmh, Table 1), i.e. the diameter that all vessels, considered as circles, in a given tissue would have to sustain exactly the same tissue hydraulic conductivity (Tyree and Zimmermann, 2002). The number of vessel was counted for primary and secondary xylems and the vessel frequency calculated by dividing this number by the surface area of the related xylem. The lumen fraction (Zanne et al., 2010) refers to the total fraction of empty holes formed by lumens. The ratio of mean vessel area to frequency (Zanne et al., 2010) as a vessel composition index, refers to the relative weight of vessel size versus vessel frequency. Many vessels could be obstructed by tyloses, so we tested for any effect of leaf size on the frequency of obstruction or the effect of obstruction on petiole conductivity. Vessel obstruction was accounted for by removing obstructed vessels from the calculations.

Data analysis

We used a prediction model to derive estimated lamina area (A_{lamina}, cm^2), since the relationship between the length of the main lobe and the undamaged lamina area is very informative ($R^2 = 0.942$, $P < 0.001$, Fig. 3). Indeed, laminae used in anatomical studies are sometimes damaged (i.e. biased lamina measurement). We derived the estimated lamina area as:

$$\textit{Estimated lamina area} = 0.701 * \textit{Main lobe length}^{2.180}$$

Only this measurement of lamina area was used to compare anatomical and morphological traits.

All statistical analyses were performed with R software (http://CRAN-R-project.org). After log transformation, the relationship between each paired trait was determined with an SMA (Standardized major axis regression; (Warton et al., 2006)), which allows measurement of the error on both the x-axis and y-axis (Harvey and Pagel, 1991). These correlation relationships are described as: $y = bx^a$, such as: $\log(y) = \log(b) + a * \log(x)$, where a is the slope (or allometric exponent) and b the intercept (allometric coefficient). A 95% confidence interval was used to decide whether it is significantly correlated or not. A slope test was performed to determine if the slope differed from 1 (H1: $a \neq 1$ for an allometric relationship) or not (H0: $a = 1$ for an isometric relationship). To avoid ambiguity when comparing p-values and decision thresholds, "P_{cor}" refers to the correlation test, and "P_{slope}" refers to the slope test (allo- or isometric relationship). SMA were carried out with the (S)MATR package (Falster et al., 2006). The lamina area prediction from the main lobe length was modeled from an NLS (non-linear least squares) with the STATS package.

A paramount *leitmotif* in our study are the scaling relationships between traits, i.e., either iso- or allometric. Indeed, the mathematical relationship has dramatic consequences for data interpretation since it has major functional implications for organism development and phylogenesis (Thompson, 1917; Huxley, 1932; Niklas, 1994). That is why these relationships are briefly examined here. A relationship is expressed as a power law equation, in which the key feature is the scaling exponent characterising the form of the relationship. In biological studies, the relationship generally refers to a size trait on the *x*-axis, whatever the level of organization (cell, tissue, organ, individual, etc.). As the absolute value of the exponent is equal to 1, the relationship is isometric: there is a strictly preserved proportional relationship between the two studied traits independently of their size. In other words, size does not affect the functional nature of the relationship. As the absolute value of the exponent is different to 1, the relationship is allometric: the proportional relationship is not preserved and the *y*-axis variable fails to keep pace with the x-axis according to the variation in size. In other words,

size affects the functional nature of the relationship depending on whether the absolute value of the exponent is greater or less than 1. In the case of a value greater than 1, the *y*-axis variable increases relatively more rapidly than the *x*-axis variable. In the course of development, the importance of the scaling exponent is such that it can be considered as a trait and a performance condition in its own right since it exhibits its own genetic basis and genetic variations and it is subject to strong heritability (Vasseur et al., 2012).

RESULTS

Morphological validation of the lamina-petiole size relationship

Overall, leaf traits were highly and positively correlated ($P < 0.001$; Table 2). There was a significant and positive correlation of allometric form among most traits (A_{pet}, L_{pet}, A_{lamina}, N_{lobe}, M_{pet}, M_{lamina}, LMA; $P_{cor} < 0.001$; $P_{slope} < 0.001$; Table 2) except for (i) A_{lamina} which was isometrically correlated with M_{lamina} ($P_{slope} = 0.210$) and (ii) LMA which was not correlated with L_{pet} and A_{lamina} ($P_{cor} > 0.05$; Table 2). PSG was not correlated with A_{pet}, N_{lobe}, M_{pet} and M_{lamina} ($P_{cor} > 0.05$; Table 2) but was negatively and allometrically correlated with the other measured traits (L_{pet}, A_{lamina}, N_{lobe}; $P_{cor} < 0.05$; $P_{slope} < 0.001$), except for LMA, which was positively correlated.

The number of lobes per lamina unit area (N_{lobe}/A_{lamina}) was negatively correlated with A_{pet} ($P_{cor} < 0.001$; Fig. 4). For a given lamina area, N_{lobes} increased with a decrease in A_{pet}.

Petiole anatomy

Petioles showed pronounced radial symmetry (Fig. 1c). The central parenchymatous pith formed the main part of the cross-section (Fig. 1c, d, e). The numerous bundles (20 to 80) were radially arranged in the pith periphery, mainly in only one cycle (Fig. 1c), but in a few cases in two cycles (Fig. 1f, g). A cambium gave rise to increments of secondary xylem internally and secondary phloem externally (Fig. 1d). The cambium showed gradual inter-petiole diversity with respect to the arrangement of the bundles. From a strictly cyclic structure to a wavy one, and at the extremity, we observed isolated bundles with complete cambium discontinuities in a more cortical position (Fig. 1f, g). Primary and secondary xylem and secondary phloem were easy to identify. Tylosis partially or totally obstructed the xylem vessels (Fig. 1d). A sub-continuous sclerenchymatous shield was present at the interface between the vascular bundles and the pith (Fig. 1d). The vascular bundles were separated by interfascicular parenchyma. Occasional sclerenchyma were present between the secondary phloem and cortical parenchyma. Depending on the extent of secondary growth, the primary

phloem was crushed between the secondary phloem and cortical parenchyma. In the most external part, there was a ring of tangential collenchyma under the epidermis, fully contiguous to the cortical parenchyma (Fig. 1d). Laticiferous canals were frequently visible, mainly in the cortex (Fig. 1f) but also in the pith, but were also sometimes completely absent. We distinguished eight component petiole tissues for further anatomical analysis (Fig. 1e): (i) the pith, (ii) the sclerenchymatous shield associated with the vascular bundles, (iii) interfascicular parenchyma, (iv) primary xylem, (v) secondary xylem, (vi) phloem (comprising primary and secondary phloem), (vii) cortical parenchyma and (viii) cortical collenchyma.

Partitioning of petiole tissue

We now describe the petiole cross-sectional area (A_{pet}) both (i) as representative of the variations in several main morphological leaf traits (A_{lamina}, M_{pet}, M_{lamina}, N_{lobe}) and (ii) as a proxy of the total leaf size; since there are strong correlations between these traits (Fig. 3; Table 2) and all the anatomical traits are described in relation to the petiole.

All the surface areas of the different tissues observed on the petiole cross-section were significantly and positively correlated with A_{pet} ($P_{cor} < 0.001$; Fig. 5a; Appendix 1). Most of the proportions of the different tissues in the petiole cross-section were significantly and positively correlated with A_{pet} ($P_{cor} < 0.01$; Fig. 5b; Appendix 1), except the primary xylem area, which represented a fixed proportion of A_{pet} (4.89 ± 0.12 %; $P_{cor} = 0.337$; Fig. 5b,c; Appendix 1). Sclerenchyma, interfascicular parenchyma, primary xylem and secondary xylem represented only small proportions of the petiole cross-section (0.00 to 3.58%; 1.71 to 7.76%; 3.50 to 5.96%; and 2.03 to 9.21%, respectively; Fig. 5b, c; Appendix 1). In contrast, pith, cortical parenchyma, phloem and collenchyma represented significant proportions of the petiole cross-section (31.90 to 59.91%; 8.84 to 29.63%; 2.15 to 17.30%; 8.49 to 23.54%, respectively; Fig. 5b,c; Appendix 1) with high variability depending on the section of the petiole concerned (Fig. 5c; Appendix 1).

A mean of 22.08 ± 1.17% of tissues was calculated for conduction including 4.89 ± 0.12% of the primary xylem, 6.96 ± 0.32% of the secondary xylem and 10.23 ± 0.99% of all the phloem (Fig. 5c; Appendix 1).

Anatomical and hydraulic considerations of the lamina-petiole size relationship

Hydraulic performances are regulated by three main parameters according to the size of the leaf: surface area of the xylem tissue, the number of vessels (N_{vessel}) and the mean hydraulic diameter (Dmh) (Fig. 6). These three traits were closely related ($P_{cor} < 0.001$), and

significantly and positively correlated with A_{pet} (P_{cor} < 0.001; Fig. 6a, b; Appendix 2). However, the frequency of the vessels (f_{vessel}, obtained by dividing the number of vessels by the xylem area; $n.mm^{-2}$) was negatively correlated with A_{pet} (P_{cor} < 0.05; Fig. 6c; Appendix 2). F was independent of xylem area (P_{cor} > 0.05; Appendix 2). S was closely correlated with A_{pet} (P_{cor} < 0.001; Fig. 6d; Appendix 2). Specifically, even for a given fixed vessel frequency, Dmh remained positively correlated with A_{pet}.

All these coordinated anatomical adjustments affect theoretical hydraulic properties. There was a positive allometric correlation between the theoretical hydraulic conductivity (K_{th}) and A_{pet} with a slope greater than 1 (P_{cor} < 0.001; P_{slope} < 0.001; Fig. 7a; Appendix 2). The same was true for A_{lamina} (P_{cor} < 0.001; Appendix 2). Overall, for each petiole, tyloses did not significantly affect K_{th}, whether we took closed vessels into account in our calculation or not, (P = 0.682). There was no correlation between petiole size and the frequency of obstruction (P = 0.636). But there was a significant difference in vessel size between obstructed and unobstructed vessels (P < 0.001) but the opposite pattern was found between primary and secondary xylem. The obstructed vessels were larger in the secondary xylem but smaller in the primary xylem. There was a high positive correlation between K_s and A_{pet} (P_{cor} < 0.001; Fig. 7b; Appendix 2): even with a given fixed xylem area, associated K_{th} increased with A_{pet}. K_{th} was also positively correlated with A_{lamina} with a slope greater than 1 (P_{cor} < 0.001; P_{slope} < 0.001; Fig 7c; Appendix 2): the larger the leaf, the more supplies go to a given lamina surface area. Moreover, K_s was positively correlated with A_{lamina} (P_{cor} < 0.001; Appendix 2).

DISCUSSION

Our study describes for the first time anatomical structures and mechanisms to better understand the nature of the first premise of Corner's rule and its underlying hydraulics and mechanical significance. Here, we discuss our three main results: (i) the shift to a leaf-level model for a rigorous functional assessment of the LSR at the intraspecific level, (ii) the pith, not the secondary xylem, as the main driver of variations in petiole size and (iii) and variations in xylem vessel anatomy, not its surface area, as the main determinant of hydraulic requirements.

Using the leaf model to extend the leaf-stem size relationship

Our results showed strong positive mainly allometric correlations between morphological traits, validating the lamina-petiole relationship as an extensive consideration of the LSR in *C.*

obtusa. Most leaf traits were related, not only internode cross-sectional area and lamina area, which are the most frequently studied (White, 1983a; b; Brouat et al., 1998; Brouat and McKey, 2001; Preston and Ackerly, 2003; Westoby and Wright, 2003; Sun et al., 2006; Normand et al., 2008; Liu et al., 2010). We found a positive and allometric correlation between A_{lamina} and A_{pet}. The form of the relationship should be interpreted with caution, in view of existing results on LSR both at intra- and interspecific levels (White, 1983a; b; Brouat et al., 1998; Brouat and McKey, 2001; Preston and Ackerly, 2003; Westoby and Wright, 2003; Sun et al., 2006; Normand et al., 2008; Liu et al., 2010). We argue that confounding intra- and interspecific levels of variation is misleading since the former relates more to developmental processes and mechanisms of adjustment, while the latter relates more to a diversity of strategies, selection pressures and evolutionary pathways. In connection with this distinction, it is interesting to note that although Sinnott's work (Sinnott, 1921) and the first premise of Corner's rule (Corner, 1949) overlap in the global frame of the LSR, Sinnott's work is more in agreement with an intraspecific and developmental perspective while Corner's formulations concern an interspecific perspective. The latter assumptions also in agreement with a recent study by (Huang et al., 2016) in which scaling models produced contrasted results between intra- and interspecific data, due to dramatic interspecific variation in stem tissue density and leaf size. Reviewing data produced by White (White, 1983a; b), who was the first to test Corner's rules across species, (Brouat et al., 1998) demonstrated an isometric LSR at the intraspecific level. However, Brouat & McKey (Brouat and McKey, 2001) found an allometric form related to the myrmecophytic habit, which is in agreement with our result. Note that even if we focus on the leaf level (lamina-petiole relationship), *C. obtusa* is a hollow-stemmed myrmecophytic tree. As discussed by Brouat & McKey (2001) in connection with the LSR, the allometric form of our lamina-petiole relationship is linked to the pith, which accounts for the largest proportion of the petiole cross-sectional area.

We complete this first point with the branching intensity-stem size trade-off. Indeed, similarly, we found a negative correlation between the number of lobes per lamina unit area and A_{pet}. For a given leaf surface, the more numerous the lamina lobes, the thinner the petiole upstream from the lamina. This result is also in agreement with Corner's rules as interpreted by (Hallé et al., 1978), as "the greater the ramification, the smaller become the branches and their appendages" (Corner, 1949). At the branched-complex level, this implies that for both fixed foliar area and photosynthetic rates (Enquist et al., 1999), the degree of branching should be a trade-off with the volume and/or density of the axes. In agreement with this hypothesis, we found a weak but significant trend to decreasing PSG for larger leaves

(notably with A_{lamina}, $P = 0.01$; Table 2). This decreasing PSG was largely driven by the proportion of pith tissue ($P < 0.001$) and underlines the significance of geometry in the support function versus the decrease in PSG in the search for lower volumetric construction costs. In the same line of thought, (Olson et al., 2009) claimed that the negative trade-off between the volume of an axis and its density is a corollary to Corner's rules and the LSR. This is in agreement with the recent work of (Trueba et al., 2016) at an intraspecific level, since leaf area was shown to be a negative trade-off with both leafing intensity and stem density according to canopy openness in a New-Caledonian woody shrub species. Interestingly, this aspect of Corner's rules applies to the leaf scale, considering lobes as counterparts of the branching process. Above all, this functional dimension (branching and leafing intensities) has rarely been studied (White, 1983a; Ackerly & Donoghue, 1998; Kleiman & Aarssen, 2007; Olson *et al.*, 2009; Osada *et al.*, 2015; Trueba *et al.*, 2016) and is far from being integrated in the leaf or global spectra of economy (Westoby et al., 2002; Westoby and Wright, 2003; Wright et al., 2004; Díaz et al., 2016), whereas it is directly linked to the optimization strategy of leaf area partitioning (Smith et al., 2017) and hence light-interception performance (Duursma et al., 2012).

Finally, the anatomy of the petiole shows characteristics that are generally associated with stem-level anatomy, like radial symmetry and secondary growth with wood. This is in agreement with the axis-like function of the petiole in the architecture of *Cecropia* (Givnish, 1984). In the context of our study, all these features strengthen the homology with a stem-like branched system and the interest of shifting to a leaf model for the rigorous functional and mechanistic assessment of the LSR, i.e. integrating anatomical and hydraulic aspects. However, secondary growth potentially implies an alteration of observed relationships and scaling with time, i.e. with the age of the leaf. This implies that secondary growth continues throughout the lifespan of the leaf, which, however could result in ambiguity with respect to secondary growth, which is generally associated with the renewal of conductive and/or supporting potentials whereas the leaves of *C. obtusa* have a relatively short lifespan (generally < 100 d). So does secondary growth continue throughout the lifespan or only during the phase of primary elongation? This question deserves further investigation in the light of mechanical requirements for or vulnerability to cavitation, for instance.

The three points (i) the positive correlation between A_{pet} and A_{lamina}, (ii) the trade-off between leaf size and lobe intensity and (iii) the axis-like anatomy of *Cecropia* petioles, call for a strong functional analogy between the LSR and the lamina-petiole relationship. This

conclusion led us to study the functional significance of anatomical adjustments in the frame of the LSR using a leaf model.

Pith, not secondary xylem, is the main driver of variations in petiole size

Variations in leaf dimensions could be the result of different processes which take place simultaneously at a macro-anatomical level or at the tissue and cell level. It seems logical that variations in petiole dimensions are primarily driven by variations in tissue surface areas and volumes. In our study, we provided a complete description of petiole anatomy for *C. obtusa* by completing a previous succinct description (Bonsen and Welle, 1983). The surface area of all the tissues we studied was found to be positively correlated with A_{pet}. However, a surprising result was that the proportions of the petiole tissue were not consistent with the leaf dimensions. Only the proportion of primary xylem to its surface area remained constant. Even if the proportion of variation in the secondary xylem can vary substantially linked to the secondary growth processes, the striking feature is the marked tendency of the variation in the pith to drive variation in the absolute size of the petiole.

Because of a high second moment of areas in flexion of more external supporting tissues (i.e. secondary xylem, sclerenchyma and collenchyma) thanks to the pith, it seems that *Cecropia* petioles have a specific and relatively cheap mechanical strategy for supporting large laminae. The key point is that the proportion of pith is positively correlated with A_{pet}, implying that the second moment of areas of external tissues is positively correlated with petiole size (under the hypothesis of conserved material properties). In other words, changing the proportion of pith with an increase in leaf size allowed for a strong structural effect (from the mechanical point of view) of support tissues (e.g. secondary xylem) as they are pushed centrifugally and since a tube is stiffer than a solid cylinder (for a given materiel and a given amount of this materiel) (Niklas, 1992). Here, more research is needed for mechanical quantification. If it holds true, this feature underlines the importance of distinguishing intra- and interspecific levels in scaling models as briefly discussed above. Indeed, here we see how a specific strategy relating to leaf size and form can determine allometric scaling.

Functional significance of anatomical adjustments by the petiole

The positive correlation we found between the leaf dimensions and K_{th} is in agreement with the results of previous studies showing that larger appendages require larger hydraulic supplies (Preston and Ackerly, 2003; Normand et al., 2008), linked to increasing evaporative demand. We also found an allometric form for this relationship, meaning that a given lamina

surface area for large leaves is supplied with disproportionate amounts of water in comparison with the supply to small leaves. This property could leads to increased evaporation and stomatal conductance but deserves more appropriate ecophysiological measurements. Anyway, this process appears to be mainly driven by an increase in the vessel diameter (derived from the mean hydraulic diameter, Dmh) rather than an increase in N_{vessel} or in the xylem area. Indeed, Dmh was positively correlated with A_{pet} whereas f_{vessel} was negatively correlated with A_{pet}. Secondary xylem area and its proportion were positively correlated with A_{pet}, but it is still difficult to discover if this process is driven by hydraulic or mechanical needs. In the same way, the K_{th} fraction supported by the secondary xylem ($P < 0.001$) upped to 66.0% and was positively correlated with A_{pet}. Here again, we are not able to state whether it is the cause or the consequence.

Overall, S was positively correlated with A_{pet}, reflecting the greater weight of variations in Dmh compared to f_{vessel} and leading to a larger petiole K_s for large leaves. Thus, xylem is hydraulically optimized through variation in Dmh, avoiding a costly and less efficient strategy which would cause more xylem tissues to grow (to support more vessels), and would result in a disproportionately large petiole relative to the lamina. This feature is in agreement with the global interspecific pattern described by Zanne *et al.* (Zanne et al., 2010). However, despite the increasing return on hydraulic performance enabled by the variation in Dmh, there must be a trade-off between Dmh and f_{vessel}. This assumption is in agreement with the theoretical model of the packing rule (Sperry et al., 2008; Chen et al., 2012), which predicts that f_{vessel} should isometrically scale with conduit size and thus allows for the area-preserving branching of vessels across different branching levels.

Furthermore, when we look carefully at the relationship between Dmh and Apet (Fig. 6b), we note that Dmh seems to reach an asymptote. Indeed, petioles larger than 100mm² exhibit a constant 80-µm-Dmh. That means that this relationship is not allometric sensus stricto an upper limit exists for Dmh. Biologically meaning, that makes sense since vessel size is constraint by the packing rule or cavitation risks (see below). In agreement with the Hagen-Poiseuille law (Tyree & Zimmerman, 2002), there is the same pattern with Ks (Fig. 7b), with petioles larger than 100mm² constraint to a Ks of ~0.05 kg•s-1•MPa-1•m-1 for total xylem. It would be of interest to extend the data for petioles larger than 100mm².

Finally, such variability calls for an investigation of vulnerability to cavitation. Indeed, Scoffoni *et al.* (2016) found that larger vessels in the leaf petiole and major veins are related to vulnerability to cavitation. In our study, we showed that larger leaves have larger vessels suggesting higher vulnerability to cavitation, which would have substantial implications for

carbon economy or for dealing with the alternation of dry and wet seasons in our study region or the potential intensification of dry seasons in Amazonia with climate change. Accordingly, we found that tyloses occur preferentially on large vessels in the secondary xylem, while tyloses are usually explained in the light of cavitation mitigation (Micco et al., 2016). Since knowledge is lacking on the intraspecific variability of vulnerability to cavitation and related factors (size, season, ontogeny), further investigations are clearly needed.

Conclusion

An extensive morphological consideration of the LSR is recommended since our study on a tree species exhibiting axis-like petioles validates the lamina-petiole relationship homologously to the LSR. By shifting to a leaf-level model, i.e. by considering the petiole to be analogous to the stem, this study showed that, at the intraspecific level, the LSR has major implications for morphology, anatomy and hydraulic functioning, all three aspects being tightly linked. However, from a morphological point of view, the hydraulic function appears to support the LSR to a lesser extent than previously thought. Indeed, variations in vessel dimensions were seen to drive xylem hydraulic performances and to avoid disproportionate petiole diameters relative to the lamina, prior to variation in the number of vessels and xylem area. Here we describe a precise mechanism for the size-related optimization of carbon allocations.

In line with the authors of recent studies (Petit et al., 2016; Sterck and Zweifel, 2016; Zhang et al., 2016), we argue that more integrated studies are needed which incorporate size-, age- and environment-related changes in the structure and function of trees. This integration should include the quantification of acquisition and transport dimensions (i.e. carbon, water, nutrients), mechanical properties and growth performance, in light of carbon economy issues, to enable the description of the precise mechanisms of adjustment. In our case, *Cecropia* trees are model tree species which, thanks to their unusual properties, enable time- and space-integrated approaches. We affirm that: (i) the relatively few botanical entities exhibited by *Cecropia* enable the entire structure and topology to be described, and allow for a complete retrospective architectural analysis; (ii) the very stable phyllochron (Heuret et al., 2002; Zalamea et al., 2008) enables accurate *a posteriori* time calibration (e.g. age of a given entity or estimation of the setting date of a given entity); (iii) *Cecropia* displays high periodicity in growth, branching and reproductive processes; (iv) the extensive distribution of some species enables intraspecific comparisons in contrasting environments (in space or over time); (v) their rapid growth makes monitoring experimental designs possible; see also (Ackerly, 1999)

and (Letort et al., 2011). The leaf level is easier to study than the stem level, but we showed that changing levels is still acceptable because in the case of *Cecropia* trees, the principles are similar. In addition, because there is no differentiation between stem categories (branch versus trunk) in *Cecropia* trees, integrating the whole tree in space and over time is relatively easy in comparison with most other species.

ACKNOWLEDGEMENTS

The authors thank Julie Bossu, Coffi Belmys Cakpo, Henri Caron, Jocelyn Cazal, Saint-Omer Cazal, Aurélie Cuvelier, Bruno Clair, Aurélie Dourdain, Jean-Yves Goret, Marie Hartwig, Ariane Mirabel, Audin Patient, Pascal Petronelli, Laurent Risser, Dylan Taxile, Valérie Troispoux, Niklas Tysklind and Lore Verryckt for their assistance with field work and measurement of leaf traits. We thank Anna Deasey for English proof reading. We thank Jacques Beauchêne, Christine Heinz and Nick Rowe for preliminary discussions around the project and first results. We thank Tancrède Alméras for critical and valuable comments on the manuscript. This study benefited from an *Investissement d'Avenir* grant managed by the *Agence Nationale de la Recherche* (CEBA, ref. ANR-10-LABX-0025).

LITERATURE CITED

ABRAMOFF, M.D., P.J. MAGALHÃES, and S.J. RAM. 2004. Image processing with ImageJ. *Biophotonics International* 11: 36–42.

ACKERLY, D. 1999. Self-shading, carbon gain and leaf dynamics: a test of alternative optimality models. *Oecologia* 119: 300–310.

ACKERLY, D., and M.J. DONOGHUE. 1998. Leaf size, sapling allometry, and Corner's rules: phylogeny and correlated evolution in maples (Acer). *The American Naturalist* 152: 767–791.

ANFODILLO, T., V. CARRARO, M. CARRER, C. FIOR, and S. ROSSI. 2006. Convergent tapering of xylem conduits in different woody species. *New Phytologist* 169: 279–290.

ANFODILLO, T., G. PETIT, and A. CRIVELLARO. 2013. Axial conduit widening in woody species: a still neglected anatomical pattern. *IAWA Journal* 34: 352–364.

BARTHELEMY, D., and Y. CARAGLIO. 2007. Plant architecture: a dynamic, multilevel and comprehensive approach to plant form, structure and ontogeny. *Annals of Botany* 99: 375–407.

BETTIATI, D., G. PETIT, and T. ANFODILLO. 2012. Testing the equi-resistance principle of the xylem transport system in a small ash tree: empirical support from anatomical analyses. *Tree Physiology* 32: 171–177.

BONSEN, K., and B.J.H. TER WELLE. 1983. Comparative wood and leaf anatomy of the Cecropiaceae (Urticales). *Bulletin du Museum national d'histoire naturelle. Section B. Adansonia, botanique, phytochimie*.

BROUAT, C., M. GIBERNAU, L. AMSELLEM, and D. MCKEY. 1998. Corner's Rules Revisited: Ontogenetic and Interspecific Patterns in Leaf-Stem Allometry. *The New Phytologist* 139: 459–470.

BROUAT, C., and D. MCKEY. 2001. Leaf-stem allometry, hollow stems, and the evolution of caulinary domatia in myrmecophytes. *New Phytologist* 151: 391–406.

BUCCI, S.J., F.G. SCHOLZ, G. GOLDSTEIN, F.C. MEINZER, and L.D.S.L. STERNBERG. 2003. Dynamic changes in hydraulic conductivity in petioles of two savanna tree species: factors and mechanisms contributing to the refilling of embolized vessels. *Plant, Cell & Environment* 26: 1633–1645.

CHAVE, J., D. COOMES, S. JANSEN, S.L. LEWIS, N.G. SWENSON, and A.E. ZANNE. 2009. Towards a worldwide wood economics spectrum. *Ecology Letters* 12: 351–366.

CHEN, H., K.J. NIKLAS, and S. SUN. 2012. Testing the packing rule across the twig–petiole interface of temperate woody species. *Trees* 26: 1737–1745.

COCHARD, H., S. COSTE, B. CHANSON, J.-M. GUEHL, and É. NICOLINI. 2005. Hydraulic architecture correlates with bud organogenesis and primary shoot growth in beech (Fagus sylvatica). *Tree Physiology* 25, 25.

CORNER, E.J.H. 1949. The Durian Theory or the Origin of the Modern Tree. *Annals of Botany* 13: 367–414.

DIAZ, S., J. KATTGE, J.H.C. CORNELISSEN, I.J. WRIGHT, S. LAVOREL, S. DRAY, B. REU, ET AL. 2016. The global spectrum of plant form and function. *Nature* 529: 167–171.

DIXON, H., and J. JOLY. 1895. On the ascent of sap. *Philosophical Transactions of the Royal Society of London*.

DUURSMA, R.A., D.S. FALSTER, F. VALLADARES, F.J. STERCK, R.W. PEARCY, C.H. LUSK, K.M. SENDALL, ET AL. 2012. Light interception efficiency explained by two simple variables: a test using a diversity of small- to medium-sized woody plants. *New Phytologist* 193: 397–408.

ENQUIST, B.J., G.B. WEST, E.L. CHARNOV, and J.H. BROWN. 1999. Allometric scaling of production and life-history variation in vascular plants. *Nature* 401: 907–911.

FALSTER, D.S., D.I. WARTON, and I.I. WRIGHT. 2006. User's guide to SMATR: Standardised Major Axis Tests & Routines Version 2.0, Copyright 2006. *R instructions*.

GIVNISH, T.J. 1984. Leaf and Canopy Adaptations in Tropical Forests. *In* Physiological ecology of plants of the wet tropics, 51–84. Dr. W. Junk Publisher, Hague.

GOURLET-FLEURY, S., J.M. GUEHL, and O. LAROUSSINE. 2004. Ecology and management of a neotropical rainforest□: lessons drawn from Paracou, a long-term experimental research site in French Guiana. Elsevier, Paris.

HACKE, U.G., R. SPICER, S.G. SCHREIBER, and L. PLAVCOVA. 2016. An ecophysiological and developmental perspective on variation in vessel diameter. *Plant, Cell & Environment*.

HAJEK, P., D. KURJAK, G. VON WÜHLISCH, S. DELZON, and B. SCHULDT. 2016. Intraspecific Variation in Wood Anatomical, Hydraulic, and Foliar Traits in Ten European Beech Provenances Differing in Growth Yield. *Frontiers in Plant Science* 7: .

HALLE, F., R.A.A. OLDEMAN, and P.B. TOMLINSON. 1978. Tropical Trees and Forests - An Architectural Analysis. Springer-Verlag Berlin Heidelberg.

HARVEY, P.H., and M.D. PAGEL. 1991. The comparative method in evolutionary biology. Oxford University Press.

HEURET, P., D. BARTHELEMY, Y. GUEDON, X. COULMIER, and J. TANCRE. 2002. Synchronization of growth, branching and flowering processes in the South American tropical tree Cecropia obtusa (Cecropiaceae). *American Journal of Botany* 89: 1180–1187.

HUANG, Y., M.J. LECHOWICZ, D. ZHOU, and C.A. PRICE. 2016. Evaluating general allometric models: interspecific and intraspecific data tell different stories due to interspecific variation in stem tissue density and leaf size. *Oecologia* 180: 671–684.

HUXLEY, J.S. 1932. Problems of Relative Growth. Methuen & Co. Ltd, London.

KLEIMAN, D., and L.W. AARSSEN. 2007. The leaf size/number trade-off in trees. *Journal of Ecology* 95: 376–382.

LENS, F., J.S. SPERRY, M.A. CHRISTMAN, B. CHOAT, D. RABAEY, and S. JANSEN. 2011. Testing hypotheses that link wood anatomy to cavitation resistance and hydraulic conductivity in the genus Acer. *The New Phytologist* 190: 709–723.

LEHNEBACH, R., R. BEYER, V. LETORT, and P. HEURET. The pipe model theory half a century on: a review. *Annals of Botany*. Available at: https://academic.oup.com/aob/advance-article/doi/10.1093/aob/mcx194/4820933 [Accessed February 1, 2018].

LETORT, V., P. HEURET, P.-C. ZALAMEA, P.D. REFFYE, and E. NICOLINI. 2011. Analysing the effects of local environment on the source-sink balance of Cecropia sciadophylla: a methodological approach based on model inversion. *Annals of Forest Science* 69: 167–180.

LIU, Z., Y. CAI, K. LI, and J. GUO. 2010. The leaf size-twig size spectrum in evergreen broadleaved forest of subtropical China. *African Journal of Biotechnology* 9: 3382–3387.

MICCO, V.D., A. BALZANO, E.A. WHEELER, and P. BAAS. 2016. Tyloses and gums: A review of structure, function and occurance of vessel occlusions. *IAWA Journal* 37: 186–205.

MILLA, R., and P.B. REICH. 2007. The scaling of leaf area and mass: the cost of light interception increases with leaf size. *Proceedings of the Royal Society of London B: Biological Sciences* 274: 2109–2115.

NICOTRA, A.B., A. LEIGH, C.K. BOYCE, C.S. JONES, K.J. NIKLAS, D.L. ROYER, and H. TSUKAYA. 2011. The evolution and functional significance of leaf shape in the angiosperms. *Functional Plant Biology* 38: 535–552.

NIINEMETS, Ü., A. PORTSMUTH, D. TENA, M. TOBIAS, S. MATESANZ, and F. VALLADARES. 2007. Do we Underestimate the Importance of Leaf Size in Plant Economics? Disproportional Scaling of Support Costs Within the Spectrum of Leaf Physiognomy. *Annals of Botany* 100: 283.

NIKLAS, K.J. 1994. Plant Allometry: The Scaling of Form and Process. University of Chicago Press.

NIKLAS, K.J. 1992. Plant Biomechanics: Engineering Approach to Plant Form and Function. University of Chicago Press, Chicago.

NORMAND, F., C. BISSERY, G. DAMOUR, and P.-É. LAURI. 2008. Hydraulic and mechanical stem properties affect leaf–stem allometry in mango cultivars. *New Phytologist* 178: 590–602.

OLSON, M.E., R. AGUIRRE-HERNANDEZ, and J.A. ROSELL. 2009. Universal foliage-stem scaling across environments and species in dicot trees: plasticity, biomechanics and Corner's Rules. *Ecology Letters* 12: 210–219.

OLSON, M.E., and J.A. ROSELL. 2013. Vessel diameter–stem diameter scaling across woody angiosperms and the ecological causes of xylem vessel diameter variation. *New Phytologist* 197: 1204–1213.

OSADA, N., E. NABESHIMA, and T. HIURA. 2015. Geographic variation in shoot traits and branching intensity in relation to leaf size in Fagus crenata: A common garden experiment. *American Journal of Botany*.

PETIT, G., T. SAVI, M. CONSOLINI, T. ANFODILLO, and A. NARDINI. 2016. Interplay of growth rate and xylem plasticity for optimal coordination of carbon and hydraulic economies in Fraxinus ornus trees. *Tree Physiology* 36: 1310–1319.

POORTER, L., and D.M.A. ROZENDAAL. 2008. Leaf size and leaf display of thirty-eight tropical tree species. *Oecologia* 158: 35–46.

PRESTON, K.A., and D.D. ACKERLY. 2003. Hydraulic architecture and the evolution of shoot allometry in contrasting climates. *American Journal of Botany* 90: 1502–1512.

ROYER, D.L., P.D. COLEY, A.D. CUTTER, K.R. JOHNSON, C.C. LABANDEIRA, A.T. MOLES, M.B. PALMER, ET AL. 2007. Fossil leaf economics quantified: calibration, Eocene case study, and implications. *Paleobiology* 33: 574–589.

SCHOLZ, A., M. KLEPSCH, Z. KARIMI, and S. JANSEN. 2013. How to quantify conduits in wood? *Frontiers in Plant Science* 4.

SCHULDT, B., C. LEUSCHNER, N. BROCK, and V. HORNA. 2013. Changes in wood density, wood anatomy and hydraulic properties of the xylem along the root-to-shoot flow path in tropical rainforest trees. *Tree Physiology* 33: 161–174.

SINNOTT, E.W. 1921. The Relation between Body Size and Organ Size in Plants. *The American Naturalist* 55: 385–403.

SMITH, D.D., J.S. SPERRY, and F.R. ADLER. 2017. Convergence in leaf size versus twig leaf area scaling: do plants optimize leaf area partitioning? *Annals of Botany* 119: 447–456.

SPERRY, J.S., F.C. MEINZER, and K.A. MCCULLOH. 2008. Safety and efficiency conflicts in hydraulic architecture: scaling from tissues to trees. *Plant, Cell & Environment* 31: 632–645.

STEPPE, K., and R. LEMEUR. 2007. Effects of ring-porous and diffuse-porous stem wood anatomy on the hydraulic parameters used in a water flow and storage model. *Tree Physiology* 27: 43–52.

STERCK, F., and R. ZWEIFEL. 2016. Trees maintain a similar conductance per leaf area through integrated responses in growth, allocation, architecture and anatomy. *Tree Physiology* 36: 1307–1309.

STEUDLE, E. 2001. The cohesion-tension mechanism and the acquisition pf water by plant roots. *Annual Review of Plant Physiology and Plant Molecular Biology* 52: 847–875.

SUN, S., D. JIN, and P. SHI. 2006. The Leaf Size–Twig Size Spectrum of Temperate Woody Species Along an Altitudinal Gradient: An Invariant Allometric Scaling Relationship. *Annals of Botany* 97: 97–107.

THOMPSON, D.W. 1917. On Growth and Form. Cambridge University Press, Cambridge.

TRUEBA, S., S. ISNARD, D. BARTHELEMY, and M.E. OLSON. 2016. Trait coordination, mechanical behavior, and growth form plasticity of Amborella trichopoda under variation in canopy openness. *AoB Plants*plw068.

TYREE, and ZIMMERMANN. 2002. Xylem Structure and the Ascent of Sap. Springer.

VASSEUR, F., C. VIOLLE, B.J. ENQUIST, C. GRANIER, and D. VILE. 2012. A common genetic basis to the origin of the leaf economics spectrum and metabolic scaling allometry. *Ecology Letters* 15: 1149–1157.

WARTON, D.I., I.J. WRIGHT, D.S. FALSTER, and M. WESTOBY. 2006. Bivariate line-fitting methods for allometry. *Biological Reviews* 81: 259–291.

WESTOBY, M., D.S. DANIEL S. FALSTER, ANGELA T. MOLES, PETER A. VESK, and AND I.J. WRIGHT. 2002. Plant Ecological Strategies: Some Leading Dimensions of Variation Between Species. *Annual Review of Ecology and Systematics* 33: 125–159.

WESTOBY, M., and I.J. WRIGHT. 2003. The Leaf Size-Twig Size Spectrum and Its Relationship to Other Important Spectra of Variation among Species. *Oecologia* 135: 621–628.

WHITE, P.S. 1983a. Corner's Rules in Eastern Deciduous Trees: Allometry and Its Implications for the Adaptive Architecture of Trees. *Bulletin of the Torrey Botanical Club* 110: 203–212.

WHITE, P.S. 1983b. Evidance that temperate east north american evergreen woody plants follow Corner's rule. *New Phytologist* 95: 139–145.

WILLIAMSON, G.B., and M.C. WIEMANN. 2010. Measuring wood specific gravity…Correctly. *American Journal of Botany* 97: 519–524.

WRIGHT, I.J., P.B. REICH, M. WESTOBY, D.D. ACKERLY, Z. BARUCH, F. BONGERS, J. CAVENDER-BARES, ET AL. 2004. The worldwide leaf economics spectrum. *Nature* 428: 821–827.

ZALAMEA, P.-C., P. HEURET, C. SARMIENTO, M. RODRIGUEZ, A. BERTHOULY, S. GUITET, E. NICOLINI, ET AL. 2012. The Genus Cecropia: A Biological Clock to Estimate the Age of Recently Disturbed Areas in the Neotropics. *PLoS ONE* 7: e42643.

ZALAMEA, P.-C., P.R. STEVENSON, S. MADRIÑAN, P.-M. AUBERT, and P. HEURET. 2008. Growth pattern and age determination for Cecropia sciadophylla (Urticaceae). *American Journal of Botany* 95: 263–271.

ZANNE, A.E., M. WESTOBY, D.S. FALSTER, D.D. ACKERLY, S.R. LOARIE, S.E.J. ARNOLD, and D.A. COOMES. 2010. Angiosperm wood structure: Global patterns in vessel anatomy and their relation to wood density and potential conductivity. *American Journal of Botany* 97: 207–215.

ZHANG, L., P. COPINI, M. WEEMSTRA, and F. STERCK. 2016. Functional ratios among leaf, xylem and phloem areas in branches change with shade tolerance, but not with local light conditions, across temperate tree species. *New Phytologist* 209: 1566–1575.

TABLES

TABLE 1. List of the morphological, anatomical and hydraulic traits analysed

Trait	Abbreviation	Unit	Formula	Reference
Ellipse surface area			$A = \pi * d_1/2 * d_2/2$ (d = diameter)	
Petiole cross-sectional area	A_{pet}	mm²		
Petiole length	L_{pet}	mm²		
Main lobe length	LM_{lobe}	cm		
Lamina area	A_{lamina}	cm²		
Number of lobes	N_{lobe}	n		
Petiole dry mass	M_{pet}	g		
Lamina dry mass	M_{lamina}	g		
Lamina mass area	LMA	g/mm^2		
Petiole specific gravity	PSG	g/mm^3		
Number of vessels	N_{vessel}	n		
Mean hydraulic diameter	Dmh	µm	$Dmh = \left(\frac{\sum D_H^4}{N}\right)^{1/4}$	Tyree & Zimmermann, 2002 (Steppe and Lemeur, 2007) Scholz *et al.*, 2013
Vessel frequency	f_{vessel}	n/mm^2	$f_{vessel} = \frac{N_{vessel}}{Xylem\ surface\ area}$	
Lumen fraction	F	%	$F = Mean\ vessel\ area * f_{vessel}$	Zanne *et al.*, 2010
Mean vessel area to density ratio	S	µm²/µm²	$S = \frac{Mean\ vessel\ area}{fvessel}$	Zanne *et al.*, 2010
Ellipse conductivity	$K_{ellipse}$	$kg \bullet s^{-}1 \bullet MPa^{-}1 \bullet m$	$K_{ellipse} = \frac{\pi}{64\eta} \frac{d_1^3 d_2^3}{d_1^2 + d_2^2}$ for $\eta = 1.002*10^{-9}$ MPa s^{-1} at 20°C	Tyree & Zimmermann, 2002 Steppe & Lemeur, 2007 Scholz *et al.*, 2013
Theoretical hydraulic conductivity	K_{th}	$kg \bullet s^{-}1 \bullet MPa^{-}1 \bullet m$	$K_{th} = \sum K_{ellipse}$	Tyree & Zimmermann, 2002 (Scholz et al., 2013)
Xylem-specific hydraulic conductivity	K_s	$kg \bullet s^{-}1 \bullet MPa^{-}1 \bullet m^{-1}$	$K_s = \frac{K_{th}}{Xylem\ surface\ area}$	Tyree & Zimmermann, 2002

TABLE 2. Correlation matrix for leaf-level morphological traits based on SMA regressions on a log-log scale.

		A_{pet}	L_{pet}	A_{lamina}	N_{lobe}	M_{pet}	M_{lamina}	LMA	PSG
x-axis	A_{pet}	-	**a 0.66*** **	**a 1.28*** **	**a 0.19*** **	**a 1.47*** **	**a 1.35*** **	**a 0.34*** **	-0.26
	L_{pet}	**0.734**	-	**a 1.90*** **	**a 0.29*** **	**a 2.26*** **	**a 2.03*** **	-0.51	**a -0.34* **
	A_{lamina}	**0.880**	**0.837**	-	**a 0.15*** **	**a 1.15*** **	**a 1.03*** **	-0.28	**a -0.22** **
	N_{lobe}	**0.186**	**0.160**	**0.139**	-	**a 7.66*** **	**a 7.03*** **	**a 1.79*** **	-1.56
	M_{pet}	**0.934**	**0.829**	**0.895**	**0.199**	-	**a 0.91*** **	**a 0.23*** **	-0.16
	M_{leaf}	**0.935**	**0.776**	**0.924**	**0.173**	**0.962**	-	**a 0.26*** **	-0.19
	LMA	**0.063**	<0.001	<0.001	**0.028**	**0.051**	**0.068**	-	**a 0.65*** **
	PSG	<0.001	**0.074**	**0.166**	0.025	0.001	<0.001	**0.334**	-

Bold values are for significant correlations ($P < 0.05$).
*: $P < 0.05$; **: $P < 0.01$; ***: $P < 0.001$

APPENDICES

Appendix 1. Correlation matrix for tissue surface area and proportion traits based on SMA regressions on a log-log scale. Allometric exponents (slopes) are presented.

	Real values		Slope	
	Proportion mean	**Proportion range**	**Surface**	**Proportion**
Pith	43.78 ± 1.51	[31.90 ; 56.91]	**a 1.17*** **	**a 0.29*** **
Sclerenchyma	2.14 ± 0.17	[0.00 ; 3.58]	**a 1.34*** **	**a 0.67*** **
Interfascicular parenchyma	3.46 ± 0.25	[1.71 ; 7.76]	**i 0.93*** **	**a -0.47*** **
Xylem I	4.89 ± 0.12	[3.50 ; 5.96]	**i 0.97*** **	-0.20
Xylem II	6.96 ± 0.32	[2.03 ; 9.21]	**a 1.13*** **	**a 0.36*** **
Phloem	10.23 ± 0.99	[2.15 ; 17.30]	**a 1.45*** **	**i 0.89** **
Cortical parenchyma	15.28 ± 1.15	[8.84 ; 29.63]	**i 0.87*** **	**a -0.50*** **
Collenchyma	13.26 ± 0.70	[8.49 ; 23.54]	**i 0.91*** **	**a -0.42** **

Bold values are for significant correlations ($P < 0.05$).
*: $P < 0.05$; **: $P < 0.01$; ***: $P < 0.001$

Appendix 2. Correlation matrix between morphological, anatomical and hydraulic traits based on SMA regressions on a log-log scale. Allometric exponent (slopes) are presented.

y-axis		*x*-axis: A_{pet}	L_{pet}	A_{lamina}	N_{lobe}	LMA_{lam}	LMA_{leaf}	PSG
A_{xyl}	TOT	**i 1.03*** **	**a 1.54*** **	**i 0.87*** **	**a 5.79** **	-3.37	**a 2.07** **	-4.20
	I	**i 0.97*** **	**a 1.41*** **	**a 0.82*** **	**a 5.38** **	-3.11	**a 1.81* **	**a -4.00* **
	II	**a 1.13*** **	**a 1.68*** **	**i 0.92*** **	**a 6.24** **	-3.67	**a 2.34** **	-4.48
N_{vessel}	TOT	**a 0.64*** **	**i 0.98*** **	**a 0.52*** **	**a 3.43*** **	**a 2.02* **	**i 1.30*** **	-2.48
	I	**a 0.56*** **	**i 0.90*** **	**a 0.48*** **	**a 3.12*** **	1.86	**i 1.13*** **	-2.32
	II	**a 0.83*** **	**i 1.22*** **	**a 0.64*** **	**a 4.30** **	2.55	**a 1.74*** **	-2.97
Dmh	TOT	**a 0.34*** **	**a 0.46*** **	**a 0.26*** **	1.92	-1.11	-0.62	-1.37
	I	**a 0.35*** **	**a 0.49*** **	**a 0.28*** **	-2.02	-1.18	-0.63	**a -1.45* **
	II	**a 0.35*** **	**a 0.45*** **	**a 0.26*** **	1.94	-1.10	-0.69	-1.35
f_{vessel}	TOT	**a -0.60*** **	**i -0.83*** **	**a -0.47*** **	-3.35	1.97	1.15	**a 2.47* **
	I	**a -0.63*** **	**i -0.89*** **	**a -0.50*** **	-3.72	2.16	1.18	**a 2.68* **
	II	**a -0.56*** **	**a -0.77*** **	**a -0.42*** **	-2.95	**a 1.71* **	0.97	**a 2.12* **
F	TOT	-0.18	-0.26	-0.14	-0.95	**a 0.61** **	**a 0.38* **	0.68
	I	-0.19	**a 0.27* **	**a 0.14* **	-1.01	0.61	-0.34	0.74
	II	0.28	-0.40	-0.21	1.43	**a 0.91** **	0.69	**i 1.03* **
S	TOT	**a 1.18*** **	**a 1.67*** **	**i 0.95*** **	6.87	-3.98	-2.25	-4.92
	I	**a 1.28*** **	**a 1.81*** **	**i 1.02*** **	7.51	-4.39	-2.33	**a -5.40* **
	II	**i 1.12*** **	**a 1.53*** **	**i 0.84*** **	6.14	-3.53	-1.99	-4.31
K_{th}	TOT	**a 1.72*** **	**a 2.35*** **	**a 1.36*** **	**a 9.85* **	-5.65	**a 3.22* **	-6.92
	I	**a 1.64*** **	**a 2.33*** **	**a 1.35*** **	9.43	-5.39	**a 2.95* **	**a -6.76* **
	II	**a 1.95*** **	**a 2.52*** **	**a 1.45*** **	**a 10.88* **	-6.17	**a 3.99** **	-7.34
K_s	TOT	**a 0.80*** **	**i 1.00*** **	**a 0.60*** **	4.31	-2.49	-1.40	-3.07
	I	**a 0.80*** **	**i 1.11*** **	**a 0.64*** **	-4.52	-2.67	-1.42	-3.29
	II	**i 0.99*** **	**i 1.17*** **	**a 0.70*** **	**a 5.06* **	-2.93	**a -1.98* **	-3.45

Lines refer to the *y*-axis while columns refer to the x-axis. Below diagonal values are regression coefficients (R^2). Bold values are for significant correlations ($P < 0.05$). a: allometric correlation ; i : isometric correlation. See Table 1 for definitions of abbreviations.
*: $P < 0.05$; **: $P < 0.01$; ***: $P < 0.001$

FIGURE LEGENDS

Fig. 1. Habits, morphological and petiole-anatomical aspects of *C. obtusa* (Urticaceae). **(A)** Habits of *C. obtusa*. **(B)** Leaf of *C. obtusa*. **(C)** Petiole cross-sectional anatomy of *C. obtusa* in the middle of the petiole. **(D)** Close-up of petiole constitutive tissues: pith (Pith), sclerenchyma (Scle), interfascicular parenchyma (Pint), primary xylem (XI), secondary xylem (XII), total phloem (Phlo), primary phloem (Phl), secondary phloem (PhII), cortical parenchyma (Pcor), collenchyma (Coll) and epidermis (Epi). Simple arrows indicate tylosed vessels. **(E)** Tissues and corresponding layer masks studied. **(F)** "Wavy" cambium with a sub-bicyclic array of vascular bundles. Arrows represent laticiferous canals. **(G)** Cambial discontinuities, island-like vascular bundles and a bicyclic array of vascular bundles.

Fig. 2. Sampling and measurement design. (a) petiole length (L_{pet}); (b) the number of lobes (N_{lobe}), here there are 7 lobes; (c) the length of the main lobe (LM_{lobe}); (d) The lamina mass area (LMA) is measured based on three tablets if a circular iron punch; (e) in the P-leaves, one segment is used to measure petiole specific gravity (PSG); (f) in the P-leaves, one segment is used for the anatomical study from which is notably derived the petiole cross-sectional area (A_{pet}); (g) the lamina surface area (A_{lamina}).

Fig. 3. (A) Relationship between the undamaged lamina area (cm^2) and the length of the main lobe (cm) based on a non-linear least square regression ($P < 0.001$; $n = 888$). An estimated lamina area can be derived from the length of the main lobe ($y = 0.90672 * x^{2.10950}$). Dashed lines represent the confidence interval at 95%. **(B)** Comparison between undamaged and measured lamina area (filled circles, dashed line; $P < 0.001$; $n = 892$) and estimated lamina area (empty circles, solid line; $P < 0.001$; $n = 1317$) corresponding to the petiole cross-sectional area. Curves are derived from the SMA regression on a log-log scale.

Fig. 4. Relationship between the ratio of the number of lobes to undamaged lamina area and the petiole cross-sectional area ($P < 0.001$). The curve is derived from the SMA regression on a log-log scale. Inset shows data on a log-log scale.

Fig. 5. (A) Relationship between the cross-sectional area of the different petiole tissues and the total petiole cross-sectional area on a log-log scale ($P < 0.001$). **(B)** Relationship between the proportions of the different tissues and the petiole cross-sectional area ($P < 0.01$). Curves are derived from the SMA regression on a log-log scale. **(C)** Boxplots of the relative

proportions of the different tissues according to the petiole cross-sectional area. Pink: pith, brown: sclerenchyma, cyan: interfascicular parenchyma, blue: primary xylem, red: secondary xylem, green: phloem, orange: cortical parenchyma, purple: collenchyma.

Fig. 6. Relationships between the petiole cross-sectional area and **(A)** the xylem surface area ($P < 0.001$), **(B)** the mean hydraulic diameter ($P < 0.001$), **(C)** the vessel frequency ($P < 0.001$), and **(D)** the ratio of mean vessel area to frequency ($P < 0.001$). Curves are derived from the SMA regression on a log-log scale. Insets show data on a log-log scale. Black: data relative the total xylem. Blue: data relative to the primary xylem. Red: data relative to the secondary xylem.

Fig. 7. Relationships between the petiole cross-sectional area and **(A)** theoretical hydraulic conductivity ($P < 0.001$), **(B)** xylem-specific hydraulic conductivity ($P < 0.001$) and **(C)** leaf-specific hydraulic conductivity ($P < 0.001$). Curves are derived from the SMA regression on a log-log scale. Insets show data on a log-log scale. Black: data relative to the total xylem. Blue: data relative to the primary xylem. Red: data relative to the secondary xylem.

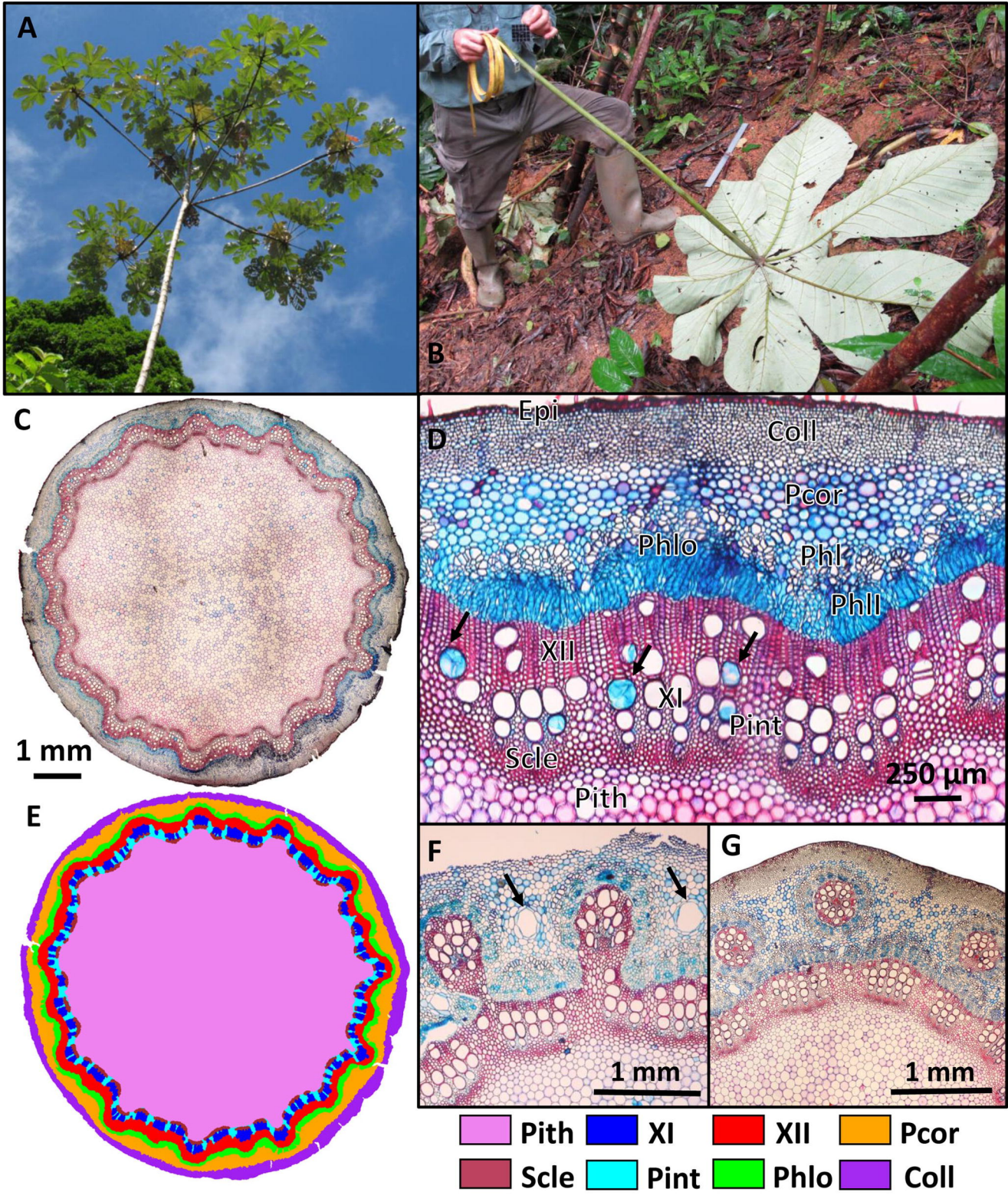
A
B
C
1 mm
D
Epi
Coll
Pcor
Phlo
Phl
PhlI
XII
XI
Pint
Scle
Pith
250 µm
E
F
1 mm
G
1 mm
Pith
XI
XII
Pcor
Scle
Pint
Phlo
Coll

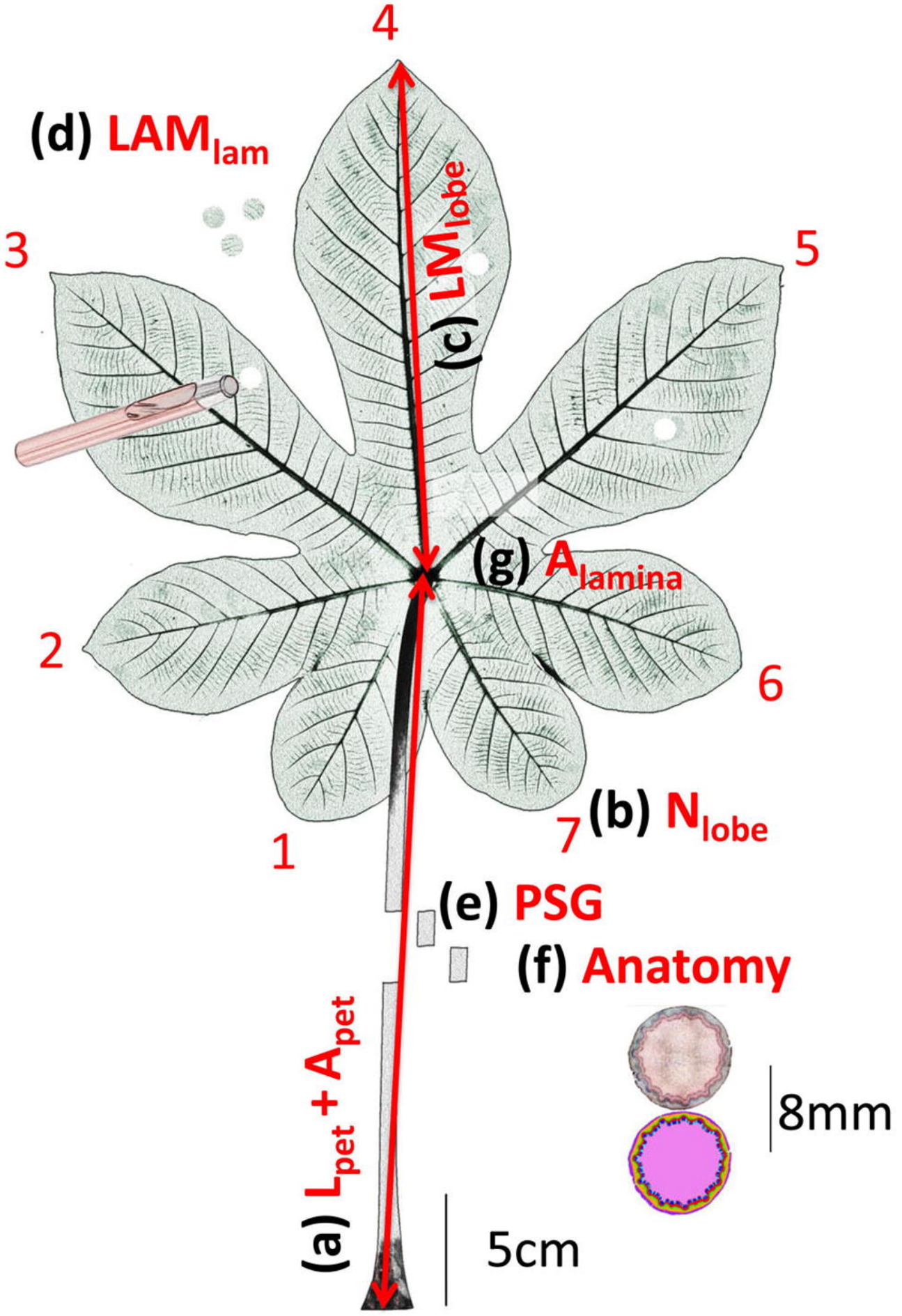
4
(d) LAM$_{lam}$
3
5
(c) LM$_{lobe}$
(g) A$_{lamina}$
2
6
7
(b) N$_{lobe}$
1
(e) PSG
(f) Anatomy
(a) L$_{pet}$ + A$_{pet}$
8mm
5cm

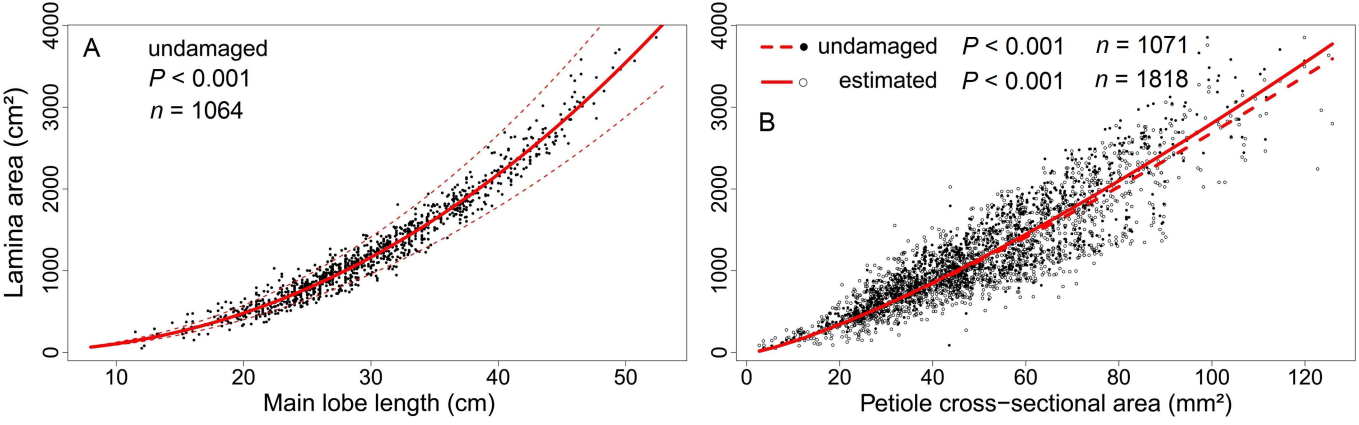
A
undamaged
P < 0.001
n = 1064
Lamina area (cm²)
Main lobe length (cm)
B
undamaged P < 0.001 n = 1071
estimated P < 0.001 n = 1818
Petiole cross−sectional area (mm²)

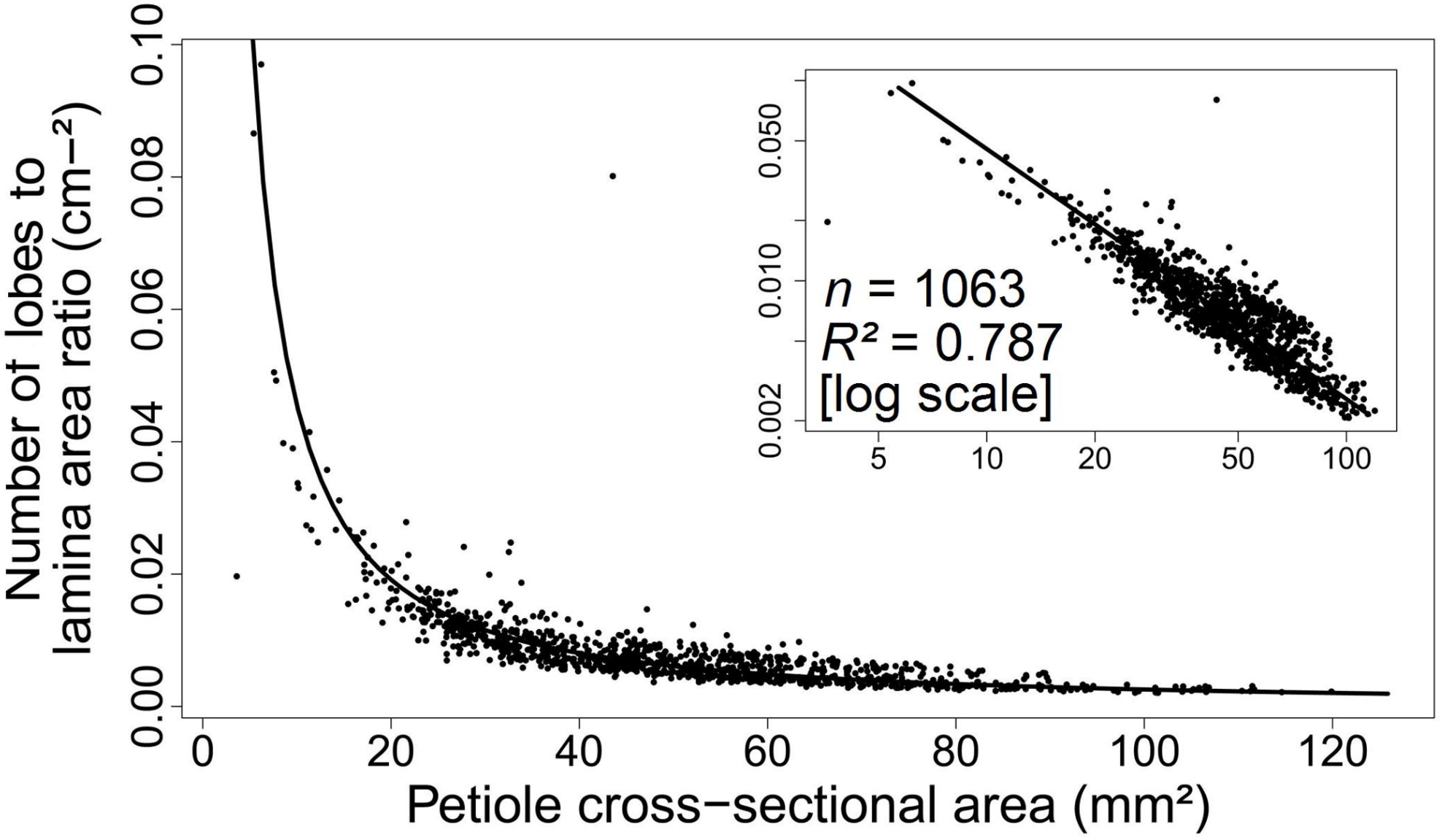
Number of lobes to lamina area ratio (cm−²)
0.00
0.02
0.04
0.06
0.08
0.10
0
20
40
60
80
100
120
Petiole cross−sectional area (mm²)
0.002
0.010
0.050
5
10
20
50
100
n = 1063
R² = 0.787
[log scale]

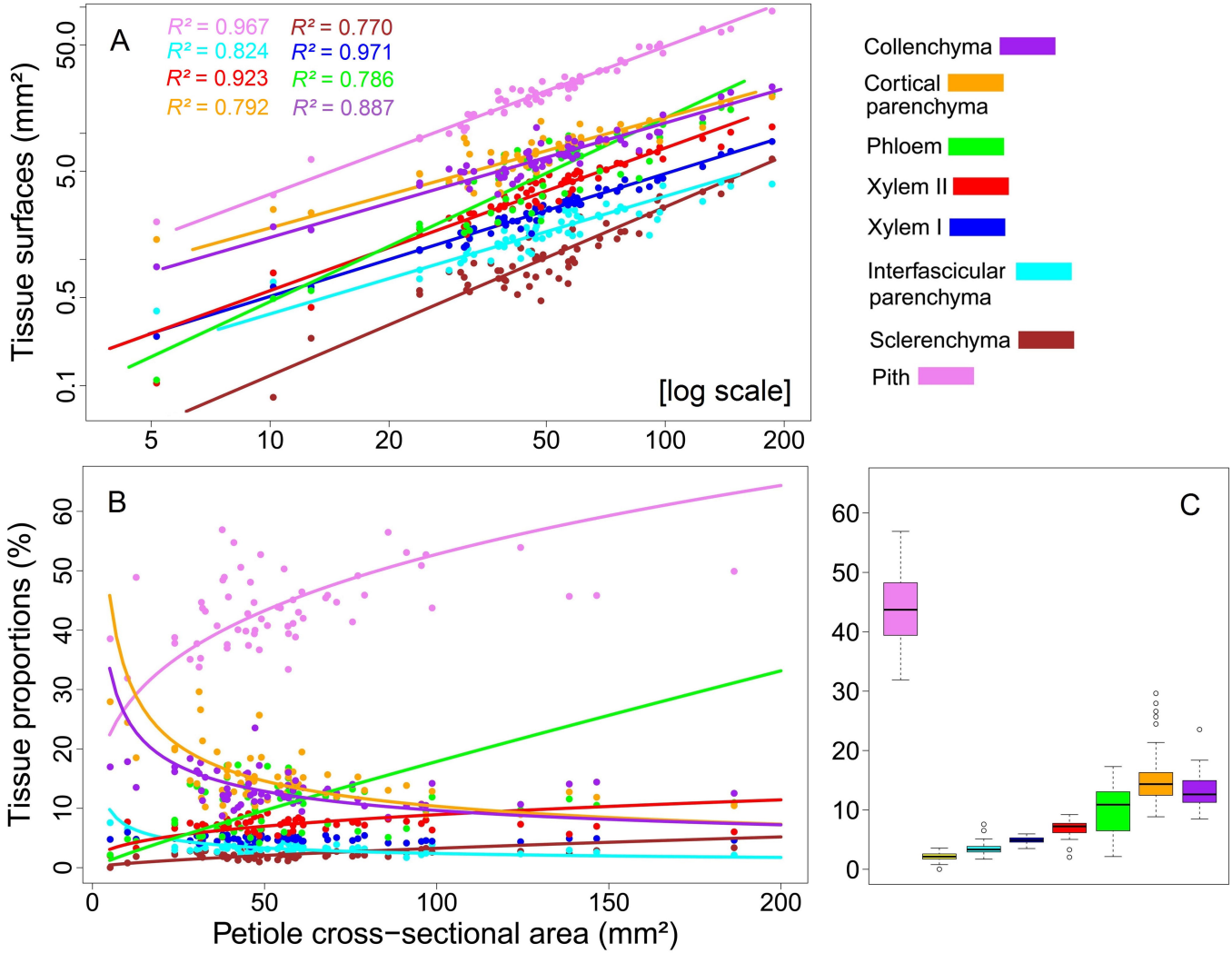
A
R^2 = 0.967
R^2 = 0.770
R^2 = 0.824
R^2 = 0.971
R^2 = 0.923
R^2 = 0.786
R^2 = 0.792
R^2 = 0.887
Tissue surfaces (mm²)
0.1
0.5
5.0
50.0
[log scale]
5
10
20
50
100
200
Collenchyma
Cortical parenchyma
Phloem
Xylem II
Xylem I
Interfascicular parenchyma
Sclerenchyma
Pith
B
Tissue proportions (%)
0
10
20
30
40
50
60
0
50
100
150
200
Petiole cross−sectional area (mm²)
C
0
10
20
30
40
50
60

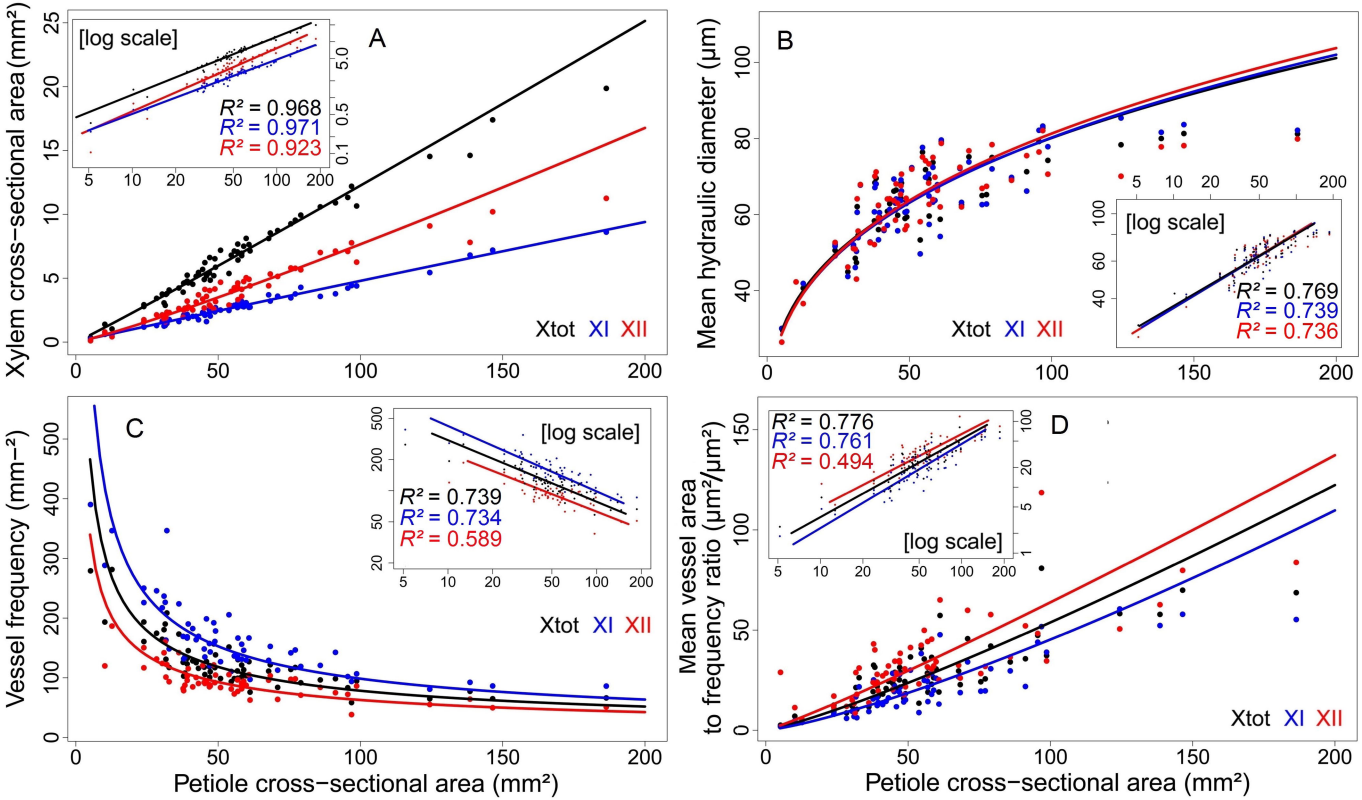
A
[log scale]
R^2 = 0.968
R^2 = 0.971
R^2 = 0.923
Xylem cross−sectional area (mm²)
Xtot XI XII
B
[log scale]
R^2 = 0.769
R^2 = 0.739
R^2 = 0.736
Mean hydraulic diameter (µm)
Xtot XI XII
C
[log scale]
R^2 = 0.739
R^2 = 0.734
R^2 = 0.589
Vessel frequency (mm−²)
Xtot XI XII
D
[log scale]
R^2 = 0.776
R^2 = 0.761
R^2 = 0.494
Mean vessel area to frequency ratio (µm²/µm²)
Xtot XI XII
Petiole cross−sectional area (mm²)
Petiole cross−sectional area (mm²)

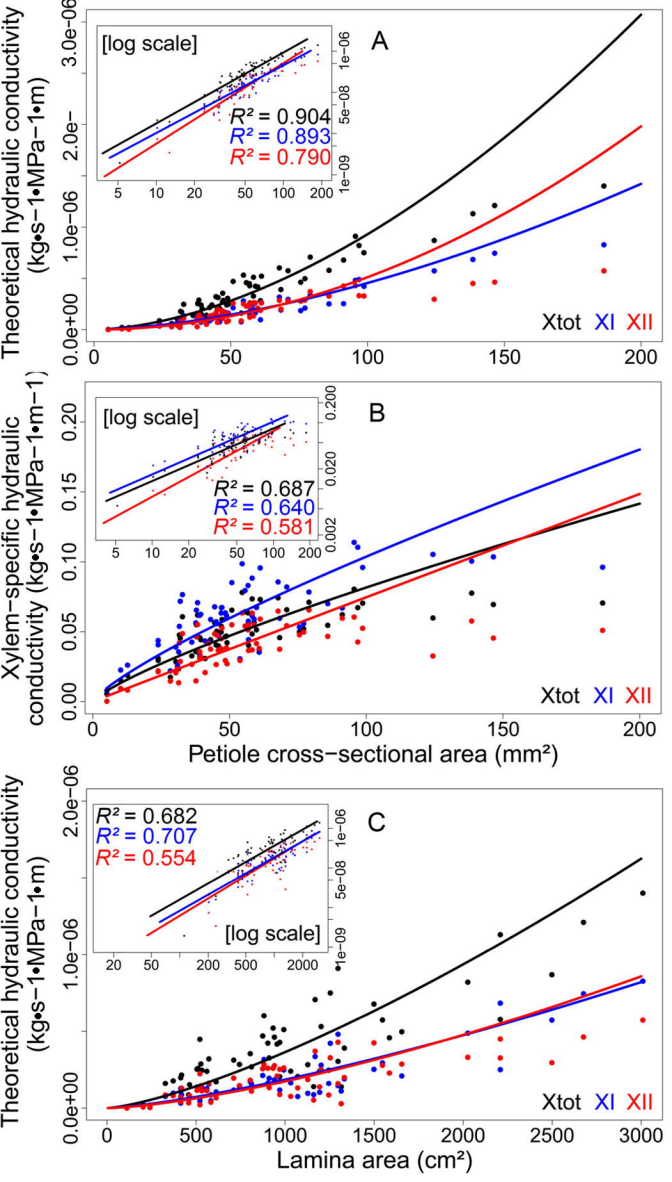
A
[log scale]
R² = 0.904
R² = 0.893
R² = 0.790
Theoretical hydraulic conductivity (kg•s−1•MPa−1•m)
Xtot XI XII
B
[log scale]
R² = 0.687
R² = 0.640
R² = 0.581
Xylem−specific hydraulic conductivity (kg•s−1•MPa−1•m−1)
Xtot XI XII
Petiole cross−sectional area (mm²)
C
R² = 0.682
R² = 0.707
R² = 0.554
[log scale]
Theoretical hydraulic conductivity (kg•s−1•MPa−1•m)
Xtot XI XII
Lamina area (cm²)